# 2P5-11

## Fabricaiton of Bone Phantoms Based on Human Bone Data and Ultrasonic Scattering Experiments

## 人骨データに基づいた骨ファントムの作製と超音波散乱実験

Takazumi Kasuga‡, Mikitsugu Nakabayashi, Takumi Otani, Shohei Nakata, and Masahiro Ohno (Chiba Institute of Technology)
春日鷹純，中林幹就，大谷拓己，中田晶平，大野正弘 (千葉工業大学)

### 1. Introduction

The number of osteoporosis patients is increasing in the aging society. Currently, standard diagnosis is performed by X-ray methods. However, ultrasonic method is also attracting attention because of its exposure-free nature and instrumentational compactness. We have been woking on creating bone phantoms that can be used in the development of ultrasonic apparatus for osteoporosis diagnosis [1-3]. For this purpose, one needs to three-dimensionally design the cancellous bone structure the bone density of which is changeable. We have so far attempted to create the cancellous bone structure by using the CT data of artifisial porous materials [1, 3], and also by purely calculating the network shapes [2, 3]. In this paper, we present the results of bone phantom fabrication using real human bone data. The ultrasonic scattering experiments for those phantoms are also described.

### 2. Fabrication of bone phantoms

We have obtained a number of HR-pQCT (High Resolution peripheral Quantitative CT) data of human radius by courtesy of the Medical School, Nagasaki University. The data were converted to stl format using commercial 3D software *mimics* (materialise). In this process, a threshold value *C* was set in the original gray-scaled DICOM CT data to binarize them to determine the position of the bone surface. Threshold *C* was set to five values (-500, -350, -200, -50 and 100) for three patients (CR02, CR04 and CR07). Higher values for *C* lead to lower bone density. **Table I** shows the structural parameters of original human bone data calculated using the software *3D-BON* (Ratoc). Among three patients, CR02 has the highest BV/TV. CR04 and CR07 have similar BV/TVs, but CR07's trabecular is sparser. The data were 3D printed by the stereolithography method (Tokyo Lithmatic corp.). The models were twice the real size. **Fig. 1** shows the fabricated bone phantoms. Models having different bone densities were realized for different three patients.

### 3. Ultrasonic scattering experiment

We have performed the experiment to obtain the images of ultrasonic field distribution transmitted through the bone phantoms. **Fig. 2**(a) shows the experimental configuration. In a water tank, tone-burst ultrasonic waves at a frequency of 2 MHz with the duration time of 20 μs were radiated from a flat transducer having the active area diameter of 12 mm. Since the phantoms are twice the real size, this condition corresponds to 4 MHz radiation onto real sized samples. Transmitted ultrasonic waves were detected by a needle-type hydrophone having a receiving area of 0.5 mm diameter (Japan Probe). By scanning the hydrophone in the *xy*-plane synchronously with

Table I. Structural parameters of original human bone data calculated by Ratoc's software *3D-BON*.

| | BV/TV | Tb.Th | Tb.N | Tb.Spac |
|---|---|---|---|---|
| | [%] | [μm] | [1/mm] | [μm] |
| CR02 TB | 13.447 | 129.9773 | 1.034565 | 822.6637 |
| CR04 TB | 10.03074 | 116.4211 | 0.861591 | 836.1293 |
| CR07 TB | 11.64812 | 161.1427 | 0.722845 | 935.9701 |

BV/TV=bone volume/total volume, Tb.Th=trabecular thickness, Tb.N=trabecular number, Tb.Spac=trabecular spacing. TB means that the values are for trabacular part only.

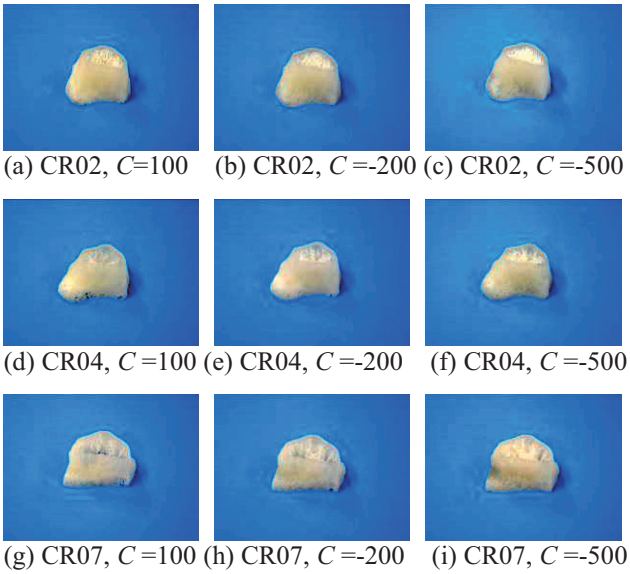

(a) CR02, *C*=100 (b) CR02, *C* =-200 (c) CR02, *C* =-500
(d) CR04, *C* =100 (e) CR04, *C* =-200 (f) CR04, *C* =-500
(g) CR07, *C* =100 (h) CR07, *C* =-200 (i) CR07, *C* =-500

Fig. 1 Bone phantoms made from human radius data. CR denotes the patients, and *C* denotes the thresholding value. Models with higher *C*s have lower bone densities.

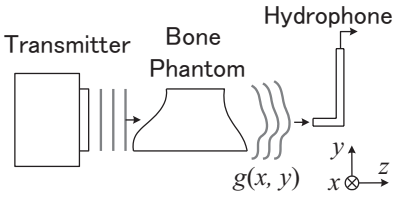


(a) Experimental configuration.

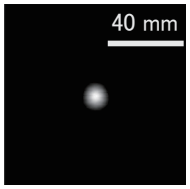


(b) no sample

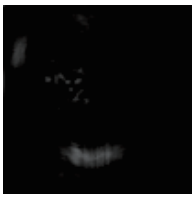

(c) CR02, $C$=-500

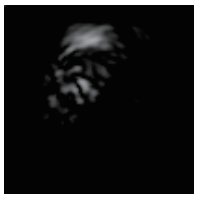

(d) CR04, $C$=-500

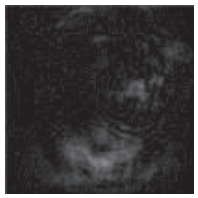

(e) CR07, $C$=-500

Fig. 2 Ultrasonic scattering experiment.

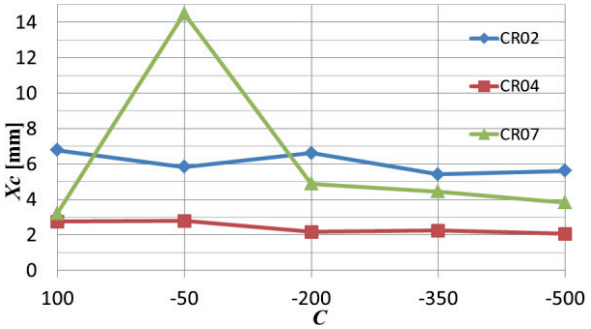


(a) Autocorrelation width $Xc$ for different $C$ values.

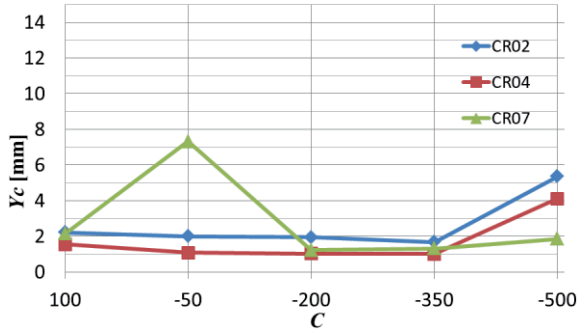


(b) Autocorrelation width $Yc$ for different $C$ values.

Fig. 3 Autocorrelation width of ultrasonic images for different $C$ values.

the ultrasonic burst, images showing ultrasonic field distribution were obtained. In this process, rf ultrasonic signals were converted to envelope detected dc signals. Fig. 2(b)-(e) show some results.

## 4. Analysis of scattered ultrasonic fields

The ultrasound may undergo strong scattering if the cancellous bone structure is made of thick and many trabeculae. Therefore, the obtained image in the above-mentioned experiment will have more complicated, grain-like structures for higher bone densities. To quantify this, we calculated the autocorrelation functions $C(X, Y)$ of obtained images $g(x, y)$. The width of the autocorrelation function around its center will be narrower for more complicated fields and thus it can be used as an index for the strength of scattering. In the following, $Xc$ denotes the separation of two points in the $X$-direction where autocorrelation value becomes smaller than its central peak by 10%, and $Yc$ in the $Y$-direction.

**Fig. 3** shows the dependence of $Xc$ and $Yc$ on the $C$ values of fabricated phantoms. The $C$ value in the 3D processing, mentioned in chapter 2, was adopted as an index for bone density, because we have not succeeded in calculating BV/TV values of only trabecular parts of fabricated phantoms. According to the theoretical forecast, values $Xc$ and $Yc$ will be larger for lower BV/TVs (larger $C$s). We see in Fig. 3(a), for sample CR07, $Xc$ increases for lower BV/TVs (larger $C$s) in the range of $-500<C<-50$, which is coherent with the forecast. However, the results for $C$=100 for CR07 is discrepant, and the results for CR02 and CR04 showed no dependence on $C$. The results for $Yc$, Fig. 4(b), were almost the same for CR07, but CR02 and CR04 show opposite dependence on $C$. As is shown, the autocorrelation analysis for the evaluation of ultrasonic scattering is not valid for these models made from real human bone samples. A possible reason is that the shape of radius has strong curves compared to the calcaneus models we formerly worked on, which may affect the ultrasonic propagation.

## 5. Conclusions

Bone phantoms were made from real human radius bone data. We have succeeded in making phantoms having different bone densities from the same site of the same patient, which may lead to mimic the osteoporotic progress in each patient. Ultrasonic scattering experiments were performed, but the autocorrelation analysis was not successful in relating the ultrasonic images to the bone density.

## Acknowledgements

The authors sincerely thank prof. K. Chiba of Nagasaki University for offering us the human bone HR-pQCT data.

## References

1. S. Nakata *et al.*: Proc. Symposium on Ultrasonic Electronics, **37**, Nov 16-18, Busan, Korea, (2016) 2P5-12.
2. S. Nakata *et al.*: Proc. Symposium on Ultrasonic Electronics, **38**, Oct 25-27, Tagajo, Japan, (2017) 1P5-14.
3. S. Nakata: IEICE Technical Report **117**(111), (June 27, 2017) US2017-21.